Carpathian Journal of Earth and Environmental Sciences, August 2020, Vol. 15, No. 2, p. 391 – 403; Doi:10.26471/cjees/2020/015/139

LANDSLIDE STUDY WITH 2D ELECTRICAL RESISTIVITY TOMOGRAPHY (ERT): A CASE STUDY FROM TURKEY

Nuray ALPASLAN[1] & Mehmet BAYRAM[2]

[1]Batman University, Faculty of Engineering and Architecture, Department of Civil Engineering, Batı Raman Campüs, 72100, Batman,Turkey, nuray.alpaslan@batman.edu.tr, ORCID: 0000-0001-6430-1222

[2]Bayram Engineering and Drilling,Soil Survey Firm, Mardin, Turkey asilbayram@hotmail.com, ORCID:0000-0002-1825-0097

Abstract: The electrical resistivity tomography (ERT) method, which has been used in the research and determination of landslides in recent years, has become more widely used with technological developments in field-data collection systems and the emergence of new algorithms for tomographic inversion. The ERT method has been applied to determine potential sliding surfaces and to reveal landslide geometry in mass movement or in areas where landslides have occurred. ERT allows scientists to solve complex geological problems such as landslides and determine the underground structure with advancements in data interpretation. Two-dimensional (2D) and three-dimensional (3D) ERT are both cheap and practical methods for providing underground images across profiles. Furthermore, multi-electrode data collection systems enable the usage of different arrays and reduce the time needed for data collection. In this study, an ERT survey was carried out in the landslide region of Ulukışla county of Niğde province. ERT data in the study area were obtained with a multi-electrode electrical resistivity system using the AGI R8 device, which can measure 8-channel 84-electrode resistivity. In the resistivity studies, six parallel 82 m long profiles were examined by using 42 electrodes, and the Dipole-Dipole-Gradient method was applied. The obtained resistivity field data were analyzed in Earthimager 2D and Earthimager 3D programs with the reverse solution process to form a model of the underground resistivity. ERT data were interpreted by conducting 2D and 3D resistivity modeling studies on the results to determine the depth, thickness, resistivity values, and water retention properties of the units.

Keywords: Landslides, Resistivity, Sliding surface, 2D-Electrical resistivity tomography (ERT)

1. INTRODUCTION

Geophysical methods have been used more commonly and widely in recent years for determining the geometries and other properties of landslides. Landslides, defined as the downhill movement of rock or soil, have different characteristics in terms of occurrence reasons and manners. Landslides are complex geological structures and displacements consisting of different layer compositions and physical property changes in the soil (Bogoslovsky & Ogilvy, 1977). It is sometimes impossible and difficult to find a solution by using known methods to reveal these complex structures. However, rapid studies can be conducted on a wide range of fields, and data with high discrimination can be produced in electrical resistivity studies, which is a geophysical method, by applying electrical resistance tomography (ERT). Two-dimensional (2D) and three-dimensional (3D) modeling electrical resistivity imaging studies have been developed to map lateral and vertical changes from the electrical resistivity method (Dahlin & Bernstone, 1997; Li & Oldenburg, 1992; Loke & Barker, 1996). In recent years, the focus has been on computer controlled multi-electrode arrays, inversion software packages, 2D and 3D data collection, and interpretation techniques as a result of new studies conducted on electrical resistivity methods due to the development of the technology. More reliable and high-resolution resistivity images were achieved with this development (Griffiths & Barker, 1993; Abdul Nassir et al., 2000; Beresnev et al., 2002; Drahor et al., 2006). The developments in the electrical resistivity method and its many advantages have facilitated the solution of various engineering problems, as well as enabling them to be applied in landslide studies. Many researchers have achieved successful results by using the electrical resistivity

method to examine landslide mechanisms (Perrone et al., 2014; Park & Kim, 2005; Drahor et al., 2006; Colangelo et al., 2008; Lee et al., 2008; Pánek et al., 2008; Shan et al., 2013). The electrical resistivity method is a widely used method for examining the lateral extension, thickness, and characteristics of landslides (Suzuki & Higashi, 2001; Batayneh & Al-Diabat, 2002; Lapenna et al., 2003; Drahor et al., 2006; Yılmaz, 2007; Lebourg et al., 2010; Yılmaz, 2011). Kılıç (2006) conducted a study on the Senirkent landslide, which is located in the city of Isparta in Turkey, to determine the thickness of the landslide material on the bedrock and the alteration zone that caused the shift by using resistivity and seismic methods. Lebourg et al., (2010) attempted to estimate the location of the sliding plane in a landslide study using the multi-electrode direct current resistivity method consisting of 24 electrodes. They used the "dipole-dipole" sequence while taking measurements from the regions near the top, middle, and buttress point in the direction perpendicular to the sliding axis of the landslide. They analyzed the results obtained from these measurements with the help of a computer program and found the pseudo-section based on the resistivity values of the measurement line. Using these sections, they have successfully determined that the sliding surface passes 12-13 m deep from the surface by taking advantage of the resistivity differences and sudden changes of the geological units.

2. STUDY AREA

The study area is located in the Ulukışla county, Niğde Province in Turkey (Fig. 1), and it is included in the Bolkar Mountains Assembly, which is a part of the Taurus Platform located in South-Central Anatolia. It is surrounded by the Taurus system in the south. The Bolkar Mountains, which have arisen with strong tectonic movements starting from the late Eocene through the early Oligocene period and entered into terrestrial environment conditions, have been cascaded by tectonic movements during the morphological evolution from the beginning of Miocene and have taken their present appearance after going through processes in different environmental conditions. Many highly developed surface and depth karstic shapes were formed on this mountainous area consisting of calcic rocks of different ages and types. Ulukışla and its surroundings generally consist of a volcanic field, and it is composed of Late Cretaceous limestone and mostly green serpentines found in the higher parts (Blumenthal, 1956).

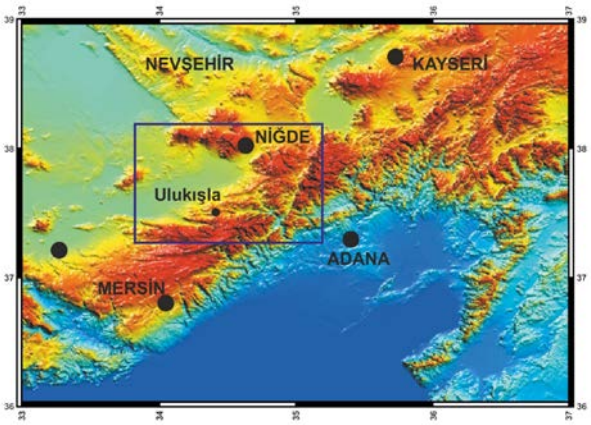

Figure 1. Study area location map.

The southern part of Ulukışla (Fig. 2) district, which is connected to the Niğde province located at the Middle Kızılırmak Area of Central Anatolia Region, is completely surrounded by the Taurus system. Bolkar Mountains are located on the part of this system called Middle Taurus. The Bolkar Mountains were partially metamorphosed in various facies environments from the beginning of Cambrian to Miocene, and consisted of sedimentary rocks that were later folded and elevated. There are relatively flat areas in the west of Ulukışla District. These flat and plain areas are mostly observed around Adana - Ankara Highway. On the other hand, river plains along the river valleys are observed in mountainous areas. The central and northern parts are of the plateau appearance.

The study area geologically consists of sedimentary, volcanic rocks and gabbro representing the Upper Cretaceous-Middle Eocene time period. It is divided into three members (Fig. 3) according to its complex lithological features. Ulukışla Formation*:* This unit formed by the volcano-sedimentary rocks was first described as the Ulukışla Group by Oktay (1973), and then later defined as the Ulukışla Formation by Demirtaşlı et al., (1975). Volcanites are commonly seen in the field as agglomerate, pillow lava, tuff, dyke, and stream breccia, and there are abundant volcanic sandstones, conglomerates, and shales alternating in places. The bottom contact of the unit is compatible and transitive to the Halkapınar Formation. The age of the fossils compiled from the sedimentary rocks of the Ulukışla Formation is Lower-Middle Eocene. Çiftehan Formation: This unit, consisting mostly of red limestone, was first defined by Demirtaşlı et al., (1975). Çiftehan Formation is the first sedimentary unit observed at the bottom of the Ereğli - Ulukışla basin. The pebble stone unit is generally represented by thin-medium layered red pelagic limestone that is incompatible with the Ophiolites. Başmakçı Limestone Member: This unit has a gray, light gray, white, partly massif,

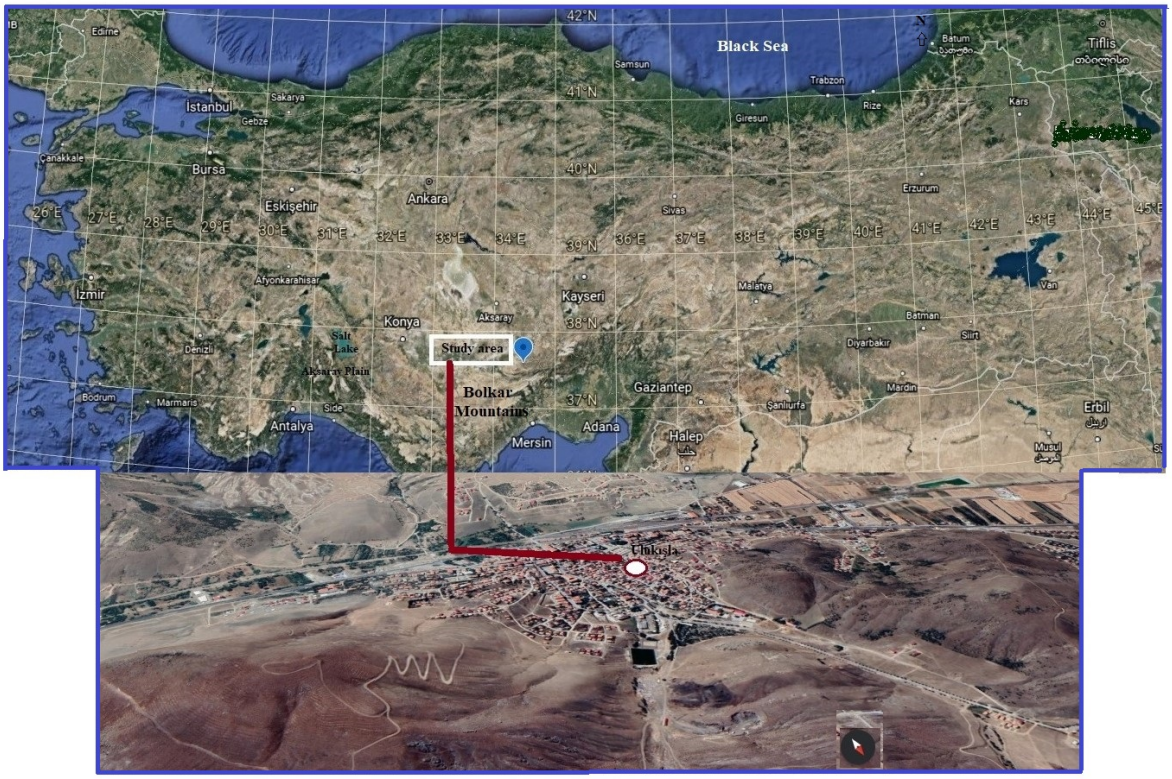

Figure 2. Geomorphological location of the study area.

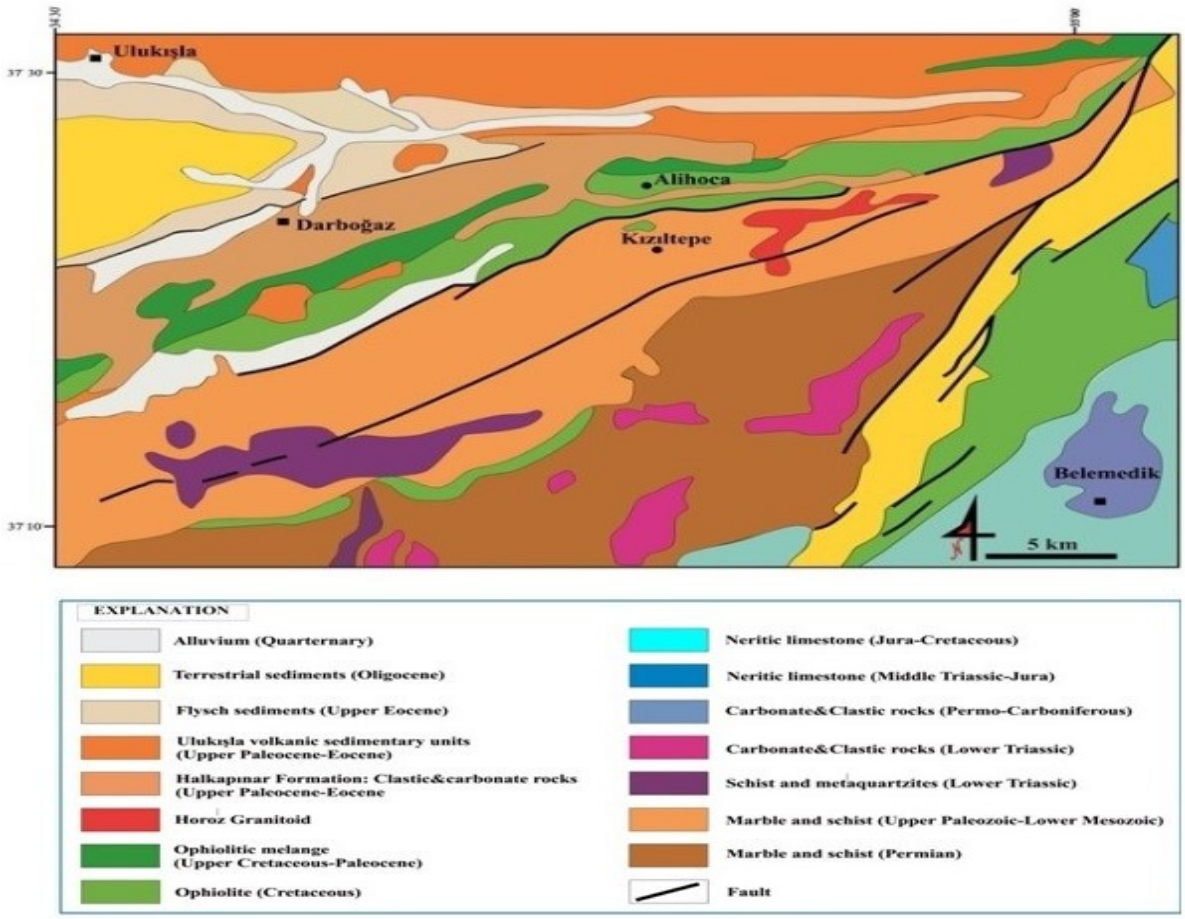

Figure 3. Geological map of the study area (Kadıoğlu & Dilek, changed from 2010).

well layered, and reefal character, and it was first defined by Blumenthal (1956). The thickness of the unit varies between 20 and 50 m. In the study area, the rocks belonging to the massif have undergone multi-phase deformation and folded due to these deformations. Ulukışla and its surroundings are generally composed of volcanic fields and contain late Cretaceous limestone and green serpentines. Furthermore, the limestone is found in higher sections. Late Permian lower marbles, late Lower-Middle Triassic schists, Ali Hoca ophiolites located in the upper cretaceous, Kalkankaya Formation with late Lower Paleocene, late Upper Paleocene - Lower Eocene granodiorite, and Deli Mahmutlu Formation with late Middle Eocene lateral rocks and late Quaternary sedimentary deposits and slope debris and alluviums are located at Bolkar Mountain and its surroundings (Demirtaşlı et al., 1975).

Figure 4.a) Close-up view and b) long-distance view of the main landslide mass.

In this study, ERT research was carried out in the landslide region (Fig. 4 a and b) within the boundaries of Ulukışla county in Niğde province. This mountainous area consists of calcic rocks of different ages and types, and highly developed surface and depth karstic shapes are formed. Therefore, there are plenty of underground drainage channels and caves that can be opened to tourism. Large stress cracks occurred in places where the sliding began on the landslide mass with the effect of water interference and the daily temperature fluctuations because the bedrock unit where the slopes are usually located is formed by serpentine, a type of faulted and fissured rock, (Fig. 5a and b), there is limestone in higher elevations, and the site is volcanic. Furthermore, the deformations occurred over time in capillary cracks caused by climatic causes, and tectonic effects in the serpentine units can be explained by the observations made in this situation. According to the 3D view of the landslide area in Figure 6, the average slope is 30-40%, the width of the crown region is 60 m, the height is approximately 18 m, and the distance between the crown and the buttress area is 50 m.

Figure 5.a) Distribution of stress cracks on the landslide mass. b) Wide-range stress cracks on the landslide mass

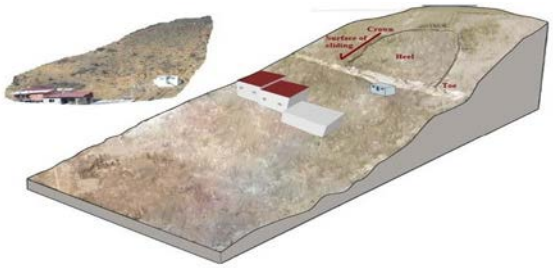
Figure 6. 3D view of the landslide mass.

3. METHODOLOGY

The electrical resistivity method is based on the principle of applying current to the soil with two electrodes using an artificial energy source and measuring the potential difference between two other electrodes. This method provides an image of the resistivity distribution underground. Resistivity is one of the variables among physical properties. Resistivity values of geological units may vary depending on their structures and the amount of water that they contain. Volcanic and metamorphic rocks have high resistivity values. The resistivity of these rocks mostly depends on the amount of faults and the percentage of the groundwater content of these faults. Sedimentary rocks, which have various clearances and high water content, usually have low resistivity. The Figure 7 shows the approximate resistivity values of common rocks.

In the application of the electrical resistivity method, arrays consisting of four electrodes, two currents (A and B), and two potential electrodes (C and D) are used. The usual electrode arrays used in resistivity measurements are shown in Figure 8. The relationship between electrical resistivity (R), current (I),and electrical potential (V) is based on Ohm's law. With the knowledge of the value of I, ΔV, and K(geometric factor, which depends on the type of array), apparent resistivity (ρ_a) of sub-surface soil can be calculated using Eq. (1) (Loke et al., 2013).

$$\rho_a = K\frac{\Delta V}{I} \quad (1)$$

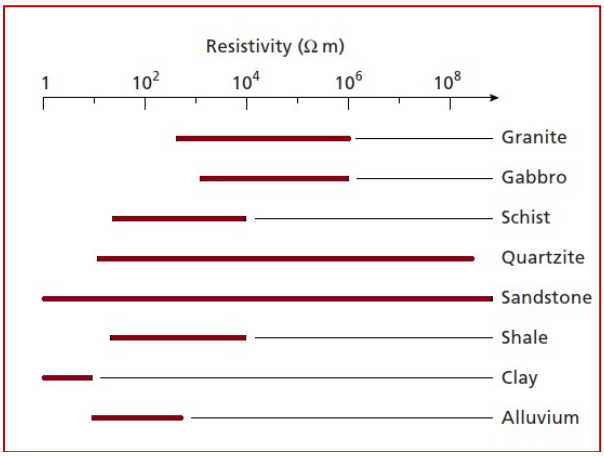

Figure 7. The approximate range of resistivity values of common rock types (Kearey et al., changed from 2002)

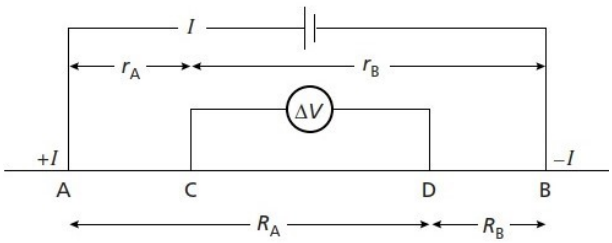

Figure 8.The generalized form of the electrode configuration used in resistivity measurements (Kearey et al., 2002)

In the resistivity method, computer-controlled data collection systems consist of the resistivity measuring instrument, the computer, a switch circuit controlling the measuring electrodes, electrode cables, their connections, and electrodes (Van Overmeeren & Ritsema, 1988; Griffiths et al., 1990; Griffiths & Barker, 1993; Dahlin, 2001). In such systems, array types, current, and the distances between the points to be measured by potential electrodes can be addressed with the help of a device and related software (Drahor et al., 2004). The underground structure can be modeled in more detail, and more information has been provided in recent years with the data-collecting multi-electrode systems. These rapid developments in the electrical method have made it possible to efficiently model 2D and 3D direct and inverse solutions (Candansayar & Başokur, 2001; Dahlin & Zhou, 2004) of complex underground structures for many different electrode arrays. It is possible to provide easy and practical information about the underground resistivity structure, both vertically and horizontally, by means of electrical resistivity imaging, which can be changed automatically to obtain drilling-profile measurements in one direction. The method includes the benefits of vertical electric drilling and profile measurement techniques (Van Overmeeren & Ritsema, 1988; Griffiths et al., 1990; Dahlin, 1996). Figure 9 shows a measurement made according to the Wenner sequence with a control module, a system consisting of a portable computer, 32 electrodes, and a multi-conductor cable. In the case of Station 1 where the electrode gaps are "a", the current electrodes are addressed as 1 and 4 while potential electrodes are addressed as 2 and 3; therefore, the process is completed by appointing the measurement of the point between 2 and 3. The same process is carried out during the new addressing that occurs by shifting each electrode once, and the process continues until the end of the profile and resistivity data are obtained for the level of n = 1.

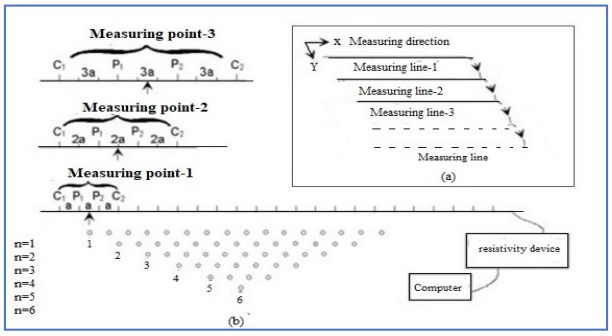

Figure 9. Multichannel resistivity measurement system and measurement stages (Griffiths & Barker, 1993)

In the study area, 2D ERT images were created with tomography measurements taken in six parallel profiles with a length of 82 m (Fig. 10 and Table 1). The structure of the landslide, its boundaries that cannot be observed on the surface, the depth of the sliding surface, the distribution order of different materials in the landslide area, the depth of the bedrock, the structure, and composition were examined. ERT is a geophysical method that can provide 2D images of the underground electrical resistance distribution (Perrone et al., 2014).

Resistivity field data received with the AGI R8 SuperSting (https://www.agiusa.com/supersting-wifi) device (Fig. 11), which can measure 8-channel 84-electrode resistivity, were analyzed in the

Figure 10. Locations of electrical resistivity profiles in the study area.

Earthimager 2D and Earthimager 3D programs. SuperSting is a multi-electrode system, and multiple electrodes are connected to the device. The device is designed to operate as dipole-dipole, pole-dipole, and pole-pole. Wenner and Schlumberger measurements can be conducted completely automatically throughout the layouts with the intelligent bidirectional automatic multi-electrode system. The choice of electrode arrays depends on the underground conditions, depth of the study, vertical and horizontal sensitivity of underground resistivity, and signal strength (Loke, 1999). In the resistivity studies, the Dipole-Dipole-Gradient method was applied. and electrodes were placed with a 2 m spacing. Forty-two electrodes were used, and six profiles were made parallel to each other.

Figure 11. SUPER STING R8 resistivity device.

4. RESULTS AND DISCUSSIONS

In this study, ERT measurements were performed along six profiles in order to determine the geometry and properties of the landslide area. In the inverse solution model section of the 2D ERT (Fig. 12 a-c) obtained for the **AA' profile (Profile 1),** the resistivity change ranges between 100,000 and 1.2 Ω-m (Fig. 12 c). In the reverse solution processes, the number of iterations is 8, and the RMS error rate is 7.69%. Three units (Fig. 12 c), indicated with different legends, were identified in the AA' model section. Blue regions represent residual units. The yellow and red regions are represented by the more compact and tighter physical units with an increase in resistivity values. Units with low resistivity values in blue regions do not pose a problem in lower elevations, but they become the most easily triggered units due to the slope effect in upper elevations. The fact that the lowest units are located in the upper elevations in this section eases the movement and decreases the slope sensitivity. The units marked with blue have higher moving potential and form the clay-containing cataclastic zone. These units move together with high seasonal precipitation and will show a continuous breaking potential from the upper units with the potential created by the slope. The lithologies found in the middle units marked with green or light blue (Fig. 12 c) are the same as the sliding units and represent units with higher density. The average depth can be estimated between 8-12 m in this region where the sliding load occurs. As the units sensitive to movement in the upper elevations transmit their load to the units in the lower levels, they will show continuous mobility due to the low slope sensitivity. In the inverse solution model section of the 2D ERT (Fig. 13 a-c) obtained for the **BB' profile (Profile 2),** the resistivity change ranges between 100,000 and 1.5 Ω-m (Fig. 13 c). In the reverse solution processes, the number of iterations is 8, and the RMS error rate is 8.16%. In the BB' model section, similar data were obtained to the ERT of AA' (Fig. 13 c), and the slope sensitivity decreased slightly compared to the sliding potential only. The average depths were identified as 10-14 m, and units capable of shifting potential were found between the 29th and 66th m. In the inverse solution model section of the 2D ERT (Fig. 14 a-c) obtained for the **CC' profile (Profile 3),** the resistivity change ranges between 100,000 and 2.2 Ω-m (Fig. 14 c). In the reverse solution processes, the number of iterations is 8, and the RMS error rate is 8.97%. When the CC 'model section was evaluated within itself (Fig. 14 c), the slope sensitivity was low with an average depth of 10 m at 45-70 m. In the inverse solution model section of the 2D ERT (Fig. 15 a-c) obtained for the **DD' profile (Profile 4),** the resistivity change ranges between 30182 and 2.0 (ohms-m) (Fig. 15 c). In the reverse solution processes, the number of iterations is 5, and the RMS error rate

Table 1. Profile line coordinates of the measurements

Line	Start		Finish		Profile length
	X	Y	X	Y	
1.Profile	36 657231	4149302	36 657247	4149217	82 meters
2.Profile	36 657207	4149286	36 657235	4149206	82 meters
3.Profile	36 657189	4149279	36 657224	4149196	82 meters
4.Profile	36 657175	4149272	36 657208	4149189	82 meters
5.Profile	36 657159	4149259	36 657200	4149181	82 meters
6.Profile	36 657145	4149246	36 657191	4149175	82 meters

Table 2. Resistivity values of the materials in the landslide

Lithology		
In the lower elevations (away from the surface)	**In the upper elevations (near the surface)**	**Resistivity value (ohm.m)**
Strict clay - Clay stone	Clay	1-20
Clayey limestone	Altered highly weathered limestone	40-400
Massive limestone	Massive limestone	400-5000
Faulted-fissured limestone	Faulted-fissured limestone	1000-5000

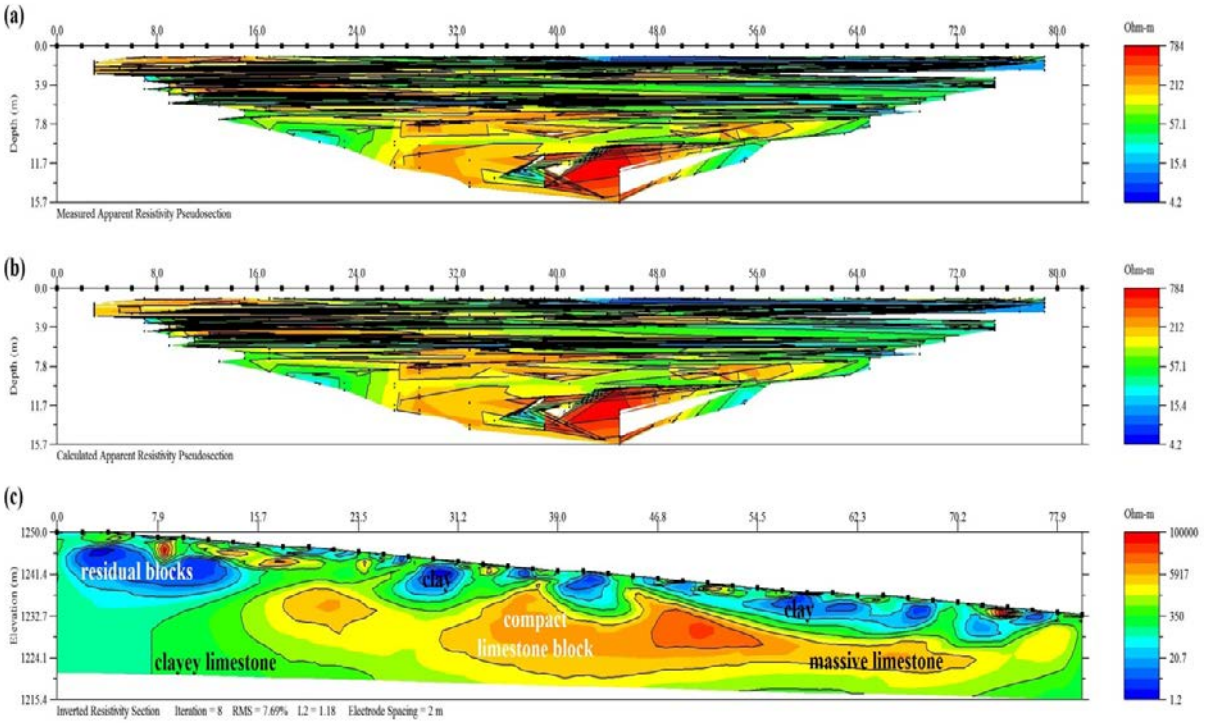

Figure 12. a) 2D underground model of AA' profile for the multi-electrode ERT study b) visible resistivity section calculated from inverse solution; and c) the transformed resistivity section

is 9.96%. In the DD' model section, there is a movement potential in the upper area at 15-38 and 55-70 m. In the inverse solution model section of the 2D ERT (Fig. 16 a-c) obtained for the **EE' profile (Profile 5),** the resistivity change ranges between 9844 and 5.3 Ω-m (Fig. 16 c). In the reverse solution processes, the number of iterations is 5, and the RMS error rate is 6.11%. According to this model section, there is not much landslide risk since the slope of the units is low, and extremely low resistivity is observed. Different results were obtained compared to the other model sections. In the inverse solution model section of the 2D ERT (Fig. 17 a-c) obtained for the **FF' profile (Profile 6),** the resistivity change ranges between 7484 and 12.1 Ω-m (Fig. 17 c). In the reverse solution processes, the number of iterations is 4, and the RMS error rate is 8.75%. As can be seen in the model section of this profile (Fig. 17 c), the movement ability of the dark blue units in the upper elevations can continuously increase with kinetic energy. Units that can cause landslides have been identified after filtering the tight and rock units and units with lowest resistivity from the measurements, and a solution is considered for the areas in this geometry. Average highest depth is 15 m, and these flows are generally estimated as 8 m.

Resistivity values of the materials forming the geological characteristics of the landslide are shown in the Table 2 according to the underground models of two-dimensional (2D) ERT results. The resistivity values of the strict clay and clay stone in the lower elevations away from the surface and the clay materials in the upper elevations near the surface are between 1 and 20 ohm.m. The resistivity values of clayey limestone at the lower elevations away from the surface and highly weathered altered limestone materials at the upper elevations near the surface are between 40 and 400 ohm.m. The resistivity values of the massive limestone material in the lower elevations

away from the surface and in the upper elevations near the surface are between 400 and 5000 ohm.m. The resistivity values of the faulted-fissured limestone material in the lower elevations away from the surface and in the upper elevations near the surface are between 1000 and 5000 ohm.m.

In general, mobility was only observed up to the first 10 m of elevations below the surface in the 3D tomography section (Fig. 18 a and b). More solid and tight units and rocks are located in the lower elevations. The dark blue units represent the altered soil. The highest mobility is observed in these areas. Furthermore, blue units will be continuously loaded with kinetic energy during the seasonal transitions due to the temperature differences of the day and night and the effect of precipitation in general.

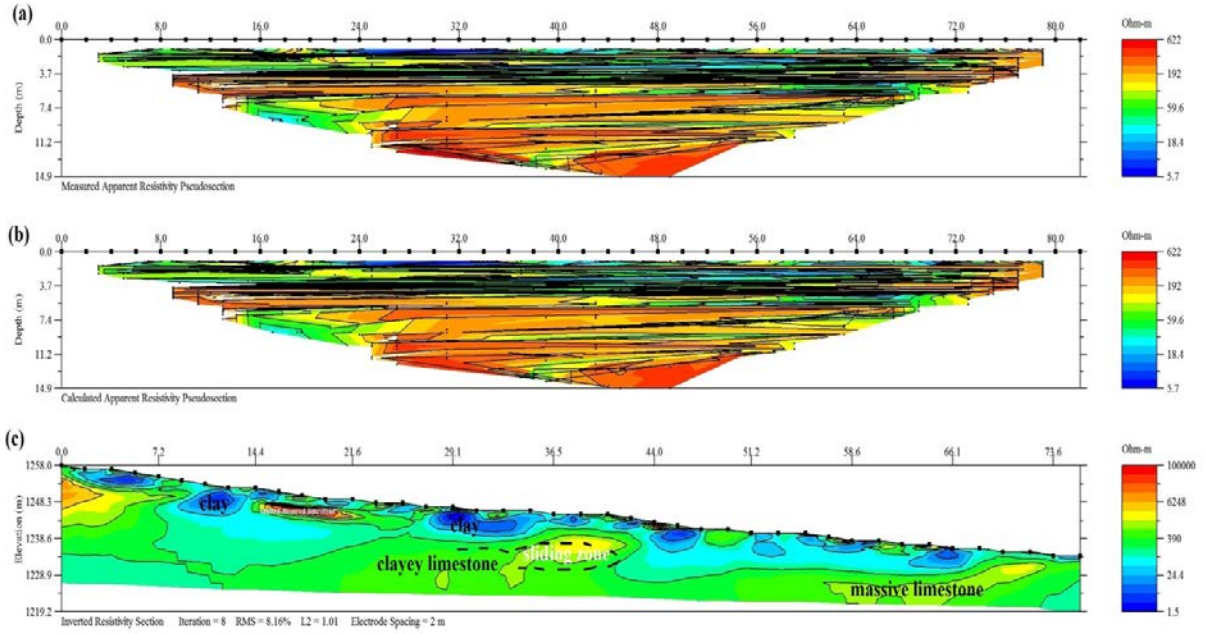

Figure 13. a) 2D underground model of BB' profile for the multi-electrode ERT study; b) visible resistivity section calculated from inverse solution; and c) the transformed resistivity section

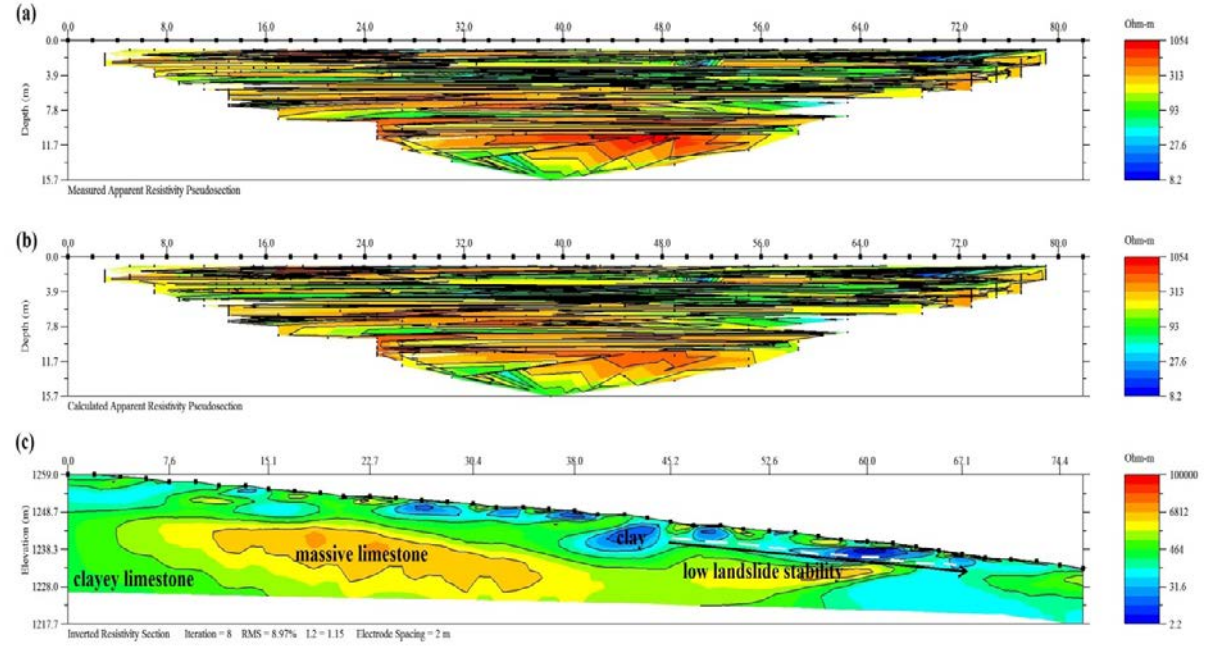

Figure 14. a) 2D underground model of CC' profile for the multi-electrode ERT study; b) visible resistivity section calculated from inverse solution; and c) the transformed resistivity section

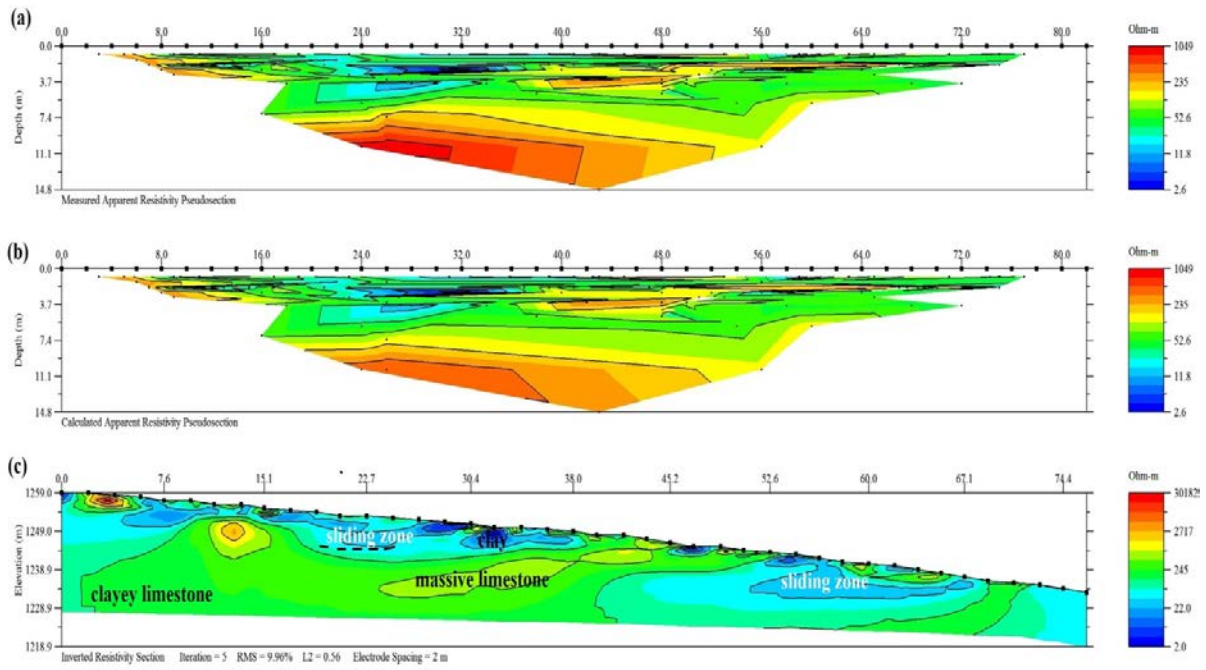

Figure 15. a) 2D underground model of DD' profile for the multi-electrode ERT study; b) visible resistivity section calculated from inverse solution; and c) the transformed resistivity section

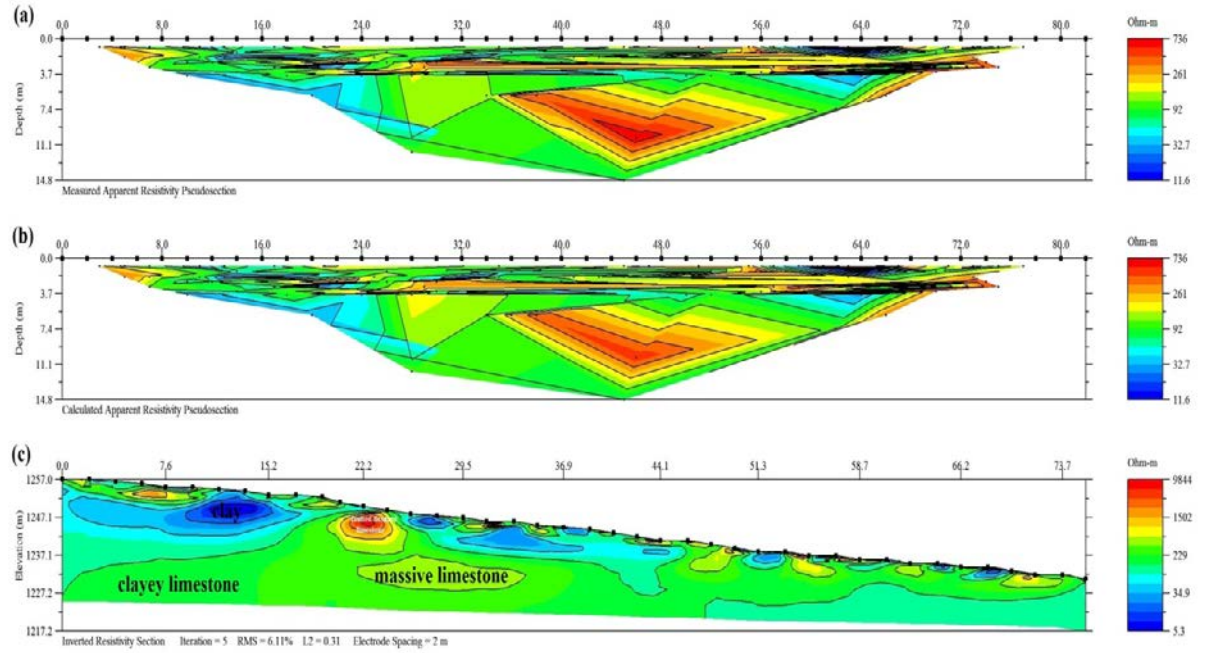

Figure 16. a) 2D underground model of EE' profile for the multi-electrode ERT study; b) visible resistivity section calculated from inverse solution; and c) the transformed resistivity section

5. CONCLUSIONS

In this study, 2D ERT model sections were evaluated for six profiles in order to reveal the importance of the ERT method in landslide studies. According to the section evaluations obtained from the measurement results: The blue regions represent the residual units, and the yellow and then red areas represent more compact and tight units with increasing resistivity values. Units with low resistivity values in the blue regions (Fig. 19) do not pose a problem in the lower elevations, but they become the most easily triggered units due to the slope effect in upper elevations.

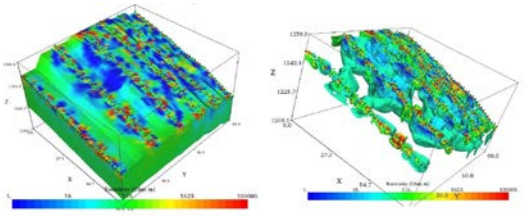

Figure 18. a) 3D Inverted resistivity image model. b) 3D Resistivity contour plot

The fact that the lowest units are located in the upper elevations in this section eases the movement while decreasing the slope sensitivity. The blue units have a larger moving potential and form the clay-containing cataclastic zone. These units move together with high seasonal precipitation and will show a continuous breaking potential from the upper units due to the potential created by the slope. The lithology of the green or light blue units is the same as the sliding units, and they represent units with higher density. When all of these factors were evaluated, we determined that the upper units are more permeable while lower units are less permeable. As a result of the conducted stability analyses, we found that the soil is unstable at points where the dark blue units are located and the slope is high, while the soil is more stable in the upper elevations where the slope is lower and the resistivity value is higher. The most important units in almost all sections are the highest elevations with very low resistivity values.

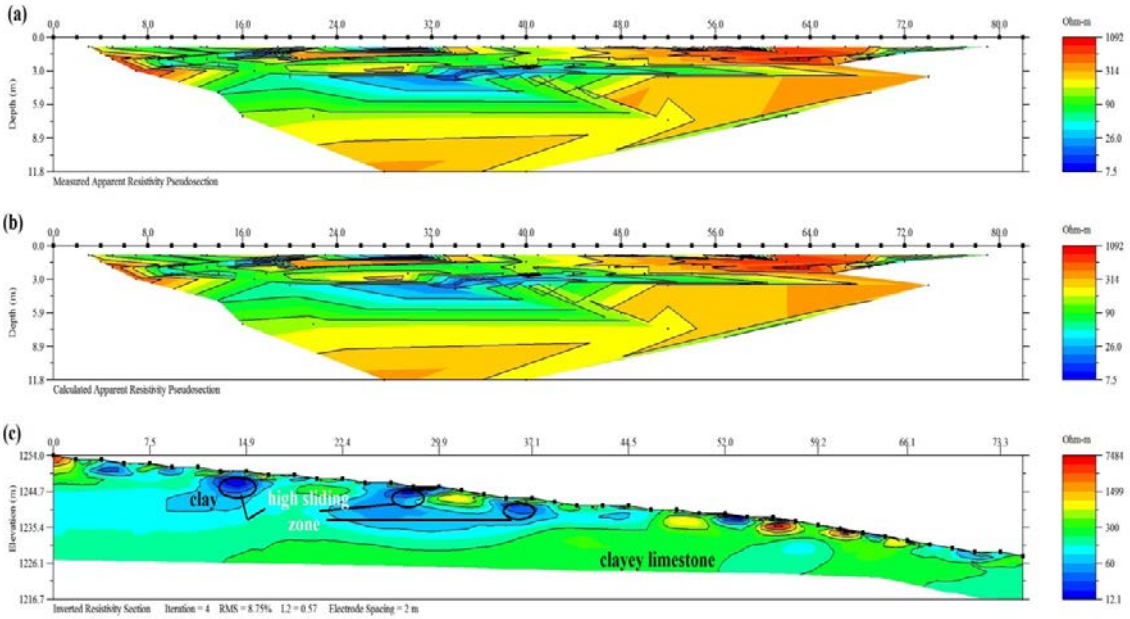

Figure 17. a) 2D underground model of FF'' profile for the multi-electrode ERT study; b) visible resistivity section calculated from the inverse solution; and c) the transformed resistivity section

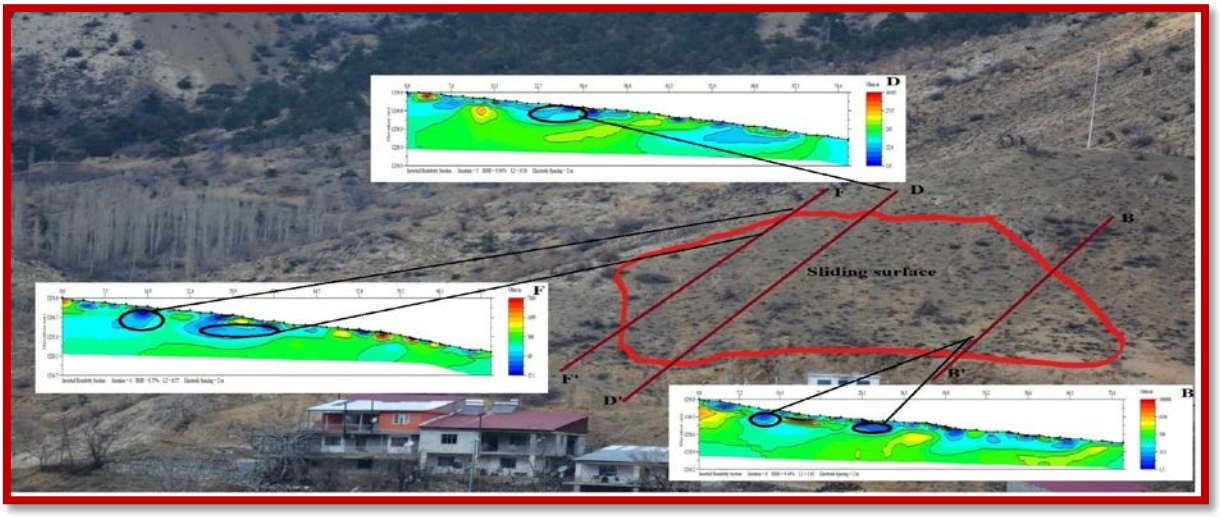

Figure 19. Potential sliding zones

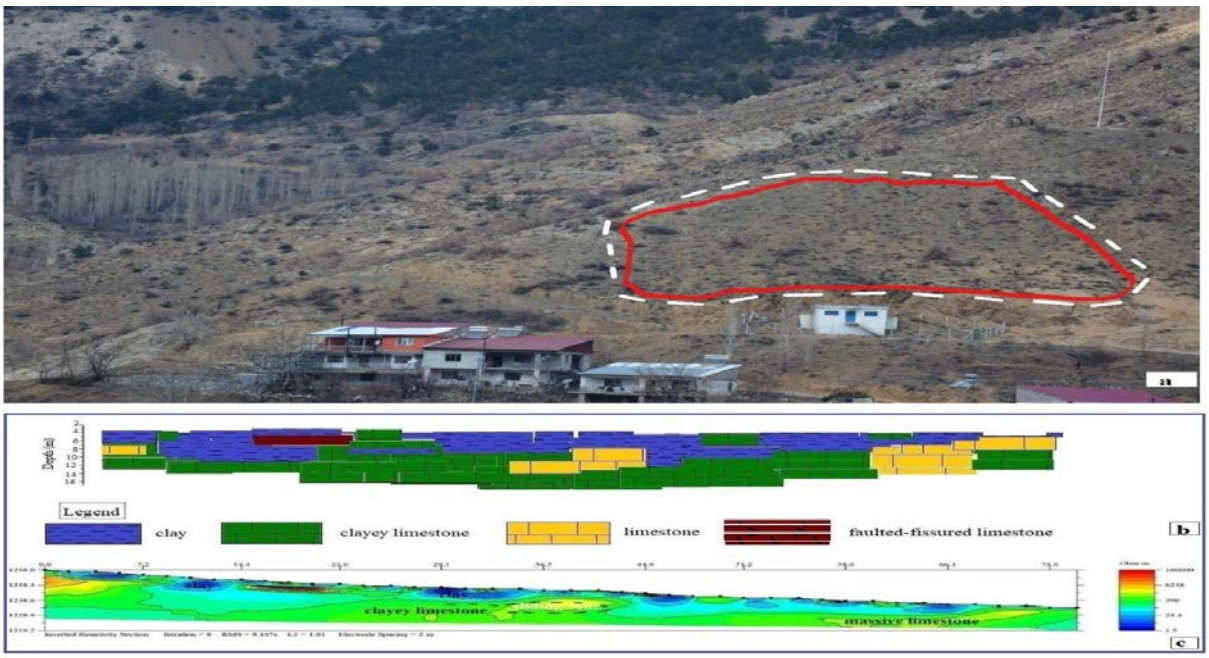

Figure 20. a) Landslide unit b) the geological section of the BB' profile c) 2D underground model of BB' profile for the transformed resistivity section.

The main problem in the slope settlements in Ulukışla and its surroundings is the risk of landslide (Fig. 20 a) even though it has a small chance of occurring. According to the electrical resistivity tomography (ERT) result, the geological section of the BB' profile is shown in Figure 20 b-c. According to the geological characteristics of the units in the study area, the clay units with multiple clearances and high water content have lower resistivity values. Clay units with low resistivity located in areas with blue legends reduce the slope sensitivity in higher elevations along with the effect of slope. Furthermore, deep and frequent decomposition of rocks observed on the clay layer due to faulted structure may increase the risk of landslides. As the soils containing limestone, which have a highly weathered, fractured and faulted structure at higher elevations, are easily weathered and splitting and falling can occur due to this weathering and depending on atmospheric conditions and tectonic effects. In the study area, highly increased surface and depth karstic forms were developed on the mountainous areas composed of calcareous rocks of different ages and types. In the places where the slope is high, the waters leaking into the limestone during the snow melting season move on the surface of the clay bands where the water contacts with clayey surfaces and appear on the surface as karstic springs. These areas also cause mass movements due to creating sliding surfaces in places where the slope is sufficient.

As a result of the studies carried out in the landslide area, the increase in the flow rate observed on the hill with snow melt in the months of heavy rainfall creates severe erosion in the buttress of the slopes, and this effect can negatively affect the stability of the slope. The stability of the slopes is compromised as a result of these movements. Therefore, it is vital to increase the stability of the slopes to be opened for use. Plants facilitate the infiltration of rainwater into the mass, slowing and reducing the surface runoff. Thus, they prevent the masses from suffering erosion. Plants with deep roots mechanically increase the balance of the masses, absorb the groundwater, and cause the masses to dry; in other words, they reduce the water content of the rocks. The lack of vegetation prevents the study area from benefiting from these positive effects in terms of stability, and there is a decrease in forces that keep the slopes in balance. Therefore, vegetation enrichment is a crucial parameter in preventing landslides in the region. However, the effect of vegetation on stability for the sliding surfaces with a depth of 15 m or above will be minimal. The weathering causes the rocks to change to a great extent and the bond between the grains to weaken and disappear completely. The rocks that have weakened due to weathering in the study area easily suffer from erosion, changing the slope angles and altitudes. As a result, the solution of active landslide problems in this region has become easier with the interpretation of the ERT results. With the ERT method, faster and more precise results can be obtained about the soil structure and units of potential landslides compared to other geotechnical methods.

REFERENCES

Abdul Nassir, S.S., Loke, M.H., Lee, C.H., & Nawawi, M.N.M., 2000. *Salt-water ġntrusion mapping by geoelectrical ımaging surveys.* Geophysical Prospecting, 48, 647–661.

Batayneh, A.T. & Al-Diabat, A.A., 2002. *Application of a two-dimensional electrical tomography technique for ınvestigating landslides along the amman-dead sea highway, Jordan.* Environmental Geology, 42, 399-403.

Beresnev, I.A., Hruby, C.E. & Davis, C.A., 2002. *The use of multi-electrode resistivity ımaging in gravel prospecting.* Journal of Applied Geophysics, 49, 245-254.

Bogoslovsky, V.A. & Ogilvy, A.A., 1977. *Geophysical methots for investigation of landslides.* Geophysics, 42, 562-571.

Blumenthal, M.M., 1956. *Geology of the northern margin regions and western extensions of the high bolkar mountain.* General Directorate of mineral research and explorations (MTA) publication, Series D, Number. 7, Ankara, 153.

Candansayar, M.E. & Başokur, A.T., 2001. *Detecting small-scale targets by the 2D inversion of two-sided three-electrode data: application to an archaeological survey.* Geophysical Prospecting, 49, 1, 40 – 53.

Colangelo, G., Lapenna, V., Loperte, A., Perrone, A. & Telesca, L., 2008, *2D electrical resistivity tomographies for investigating recent activation landslides in Basilicata Region (Southern Italy)*, Annals of Geophysics, 51, 275–285;

Dahlin, T., 1996. 2D *Resistivity Surveying for Environmental and Engineering Applications.* First Break, 14, 275-284.

Dahlin, T. & Bernstone, C., 1997. *A roll-along technique for 3D resistivity data acquisition with multi-electrode arrays, procs.* SAGEEP'97 (Symposium on the Application of Geophysics to Engineering and Environmental Problems), 23-26 March, Reno, Nevada, 927-935.

Dahlin, T., 2001. *The development of DC resistivity imaging techniques. Department of Geotechnolog,* Lund University, Box 118, S-221 00 Lund, Sweden.

Dahlin, T. & Zhou, B., 2004. *A numerical comparison of 2-D resistivity ımaging with 10 electrode arrays.* Geophysical Prospecting, 52, 379-398.

Demirtaşlı, E., Turhan, N., Bilgin, A.Z. & Selim, M., 1975. *The geology of the Bolkar Mountains:* 50th Anniversary of the Republic Earth Sciences Congress Declarations, 42-58.

Drahor, M.G., Göktürkler, G., Berge, M.A. & Kurtulmuş, T.Ö., 2004. *Visible resistivity modeling of some three dimensional shallow underground structures according to four different electrode arrays.* Hacettepe University Earth Sciences application and research center journal, Earth sciences, 30, 115-128.

Drahor, M.G., Göktürkler, G., Berge, M.A., Kurtulmus, T.Ö., 2006. *Application of electrical resistivity tomography technique for ınvestigation of landslides: A case from Turkey.* Environmental Geology, 50, 147–155.

Griffiths, D.H., Turnbull, J. & Olayinka, A.I., 1990. *Two-dimensional resistivity mapping with a computer-controlled array*. First Break, 8, 4, 121–129.

Griffiths, D. H. & Barker R.D., 1993. *Two-dimensional resistivity ımaging and modelling in areas of complex geology.* Journal of Applied Geophysics, 29, 211-226.

Kadıoğlu, Y. & Dilek, Y., 2010. *Structure and geochemistry of the adakitik Horoz granitoid, Bolkar Mountains, south-central Turkey, and its tectonomagmatic evolution*. International Geology Review, 52, 505- 535.

Kearey P., Brooks M. & Hill I., 2002. *An introduction to geophysical exploration,* 3rd Edition. Blackwell, Oxford, 184-185.

Kılıç, A., 2006. *Investigation of senirkent landslide area with resistivity and seismic methods*. Master. thesis, Univ.of Süleyman Demirel, 56.

Lapenna, V., Lorenzo, P., Perrone, A., Piscitelli, S., Sdao, F. & Rizzo, E., 2003. *High resolution geoelectrical tomographies in the study of Giarrossa landslide (Southern Italy).* Bulletin of Engineering Geology and the Environment, 62, 259-268

Lee, C.-C., Yang, C.-H., Liu, H.-C., Wen, K.-L., Wang, Z.-B. & Chen, Y.-J., 2008. *A Study of the hydrogeological environment of the lishan landslide area using resistivity image profiling and borehole data*. Engineering Geology, 98, 3, 115-125;

Lebourg, T., Hernandez, M., Zerathe, S., El Bedoui, S., Jomard, H. & Fresia, B., 2010. *Landslides triggered factors analyzed by time lapse electrical survey and multidimensional statistical approach.* Engineering Geology, 114, 238-250

Li, Y. & Oldenburg D.W., 1992. *Approximate ınverse mappings in DC resistivity problems.* Geophysical Journal International, 109, 343-362.

Loke, M. H. & Barker, R.D., 1996. *Rapid least-squares ınversion of apparent resistivity pseudosections using a quasi-newton method.* Geophysical Prospecting, 44, 131-152.

Loke, M. H., 1999. *Electrical imaging surveys for environmental and engineering studies. A practical guide to 2-D and 3-D surveys,* 66.

Loke M.H, Chambers J.E, Rucker D.F, Kuras O. & Wilkinson P.B., 2013. *Recent developments in the direct-current geoelectrical imaging method.* J Appl Geophys, 95, 135–156.

Oktay, F. Y., 1973. *Sedimentary and tectonic history of the Ulukışla area, southern Turkey.* PhD. thesis, Univ. of London, 414.

Park, S.-G. & Kim, J.-H., 2005. *Geological survey by electrical resistivity prospecting in landslide area*. Geosystem Engineering, 8, 2, 35-42.

Pánek, T., Hradecký, J. & Šilhán, K., 2008. *Application of electrical resistivity tomography (ERT) in the study of various types of slope deformations in anisotropic bedrock: case studies from the Flysch Carpathians*. Evolution, 42, 57-73.

Perrone, A., Iannuzzi, A., Lapenna, V., Lorenzo, P., Piscitelli, S., Rizzo, E. & Sdao, F., 2014. *High-resolution electrical imaging of the Varco d'Izzo earthflow (Southern Italy).* Journal of Applied Geophysics, 56, 1, 17-29.

Shan, W., Hu, Z., Jiang, H., Guo, Y. & Wang, C., 2013. *Mechanism of permafrost landslide based on GPS and resistivity surveying*, Progress of Geo-Disaster Mitigation Technology in Asia, Springer, 349-361.

Suzuki K, & Higashi S., 2001. *Groundwater flow after heavy rain in landslide-slope area from 2-D ınversion of resistivity monitoring data.* Geophysics, 49, 1708-1717.

Van Overmeeren, R.A. & Ritsema, I.L., 1988. *Continuous vertical electrical sounding.* First Break, 6, 10, 313–324.

Yılmaz, S., 2007. *Investigation of Gürbulak landslide using 2D electrical resistivity image profiling method (Trabzon, Northeastern Turkey).* Journal of Environmental & Engineering Geophysics, 12, 199-205.

Yılmaz, S., 2011. *A case study of the application of electrical resistivity ımaging for ınvestigation of a landslide along highway.* International Journal of Physical Sciences, 6, 5843-5849.

Received at: 22. 05. 2020
Revised at: 12. 08. 2020
Accepted for publication at: 14. 08. 2020
Published online at: 17. 08. 2020